Int J Adv Eng Sci Appl Math (September 2010) 2(3):119–124
DOI 10.1007/s12572-011-0024-0

IIT, Madras

ORIGINAL RESEARCH

Application of a kinematic-cyclic plasticity model in simulating sand liquefaction

Yu Bao · Stein Sture

Published online: 9 March 2011

Abstract The mechanical behavior of saturated soil is mainly governed by the interaction between the soil skeleton and the pore fluid, and this interaction may lead to significant loss of strength known as liquefaction under seismic loading conditions. The main objective of this paper is to implement a cyclic constitutive model based on fuzzy set plasticity theory, which is capable of modeling soil dilatancy during earthquake excitation. A numerical study of sand liquefaction was performed and compared with centrifuge-based experimental results. The proposed formulation is capable of capturing the features of pore water pressure buildup and strength loss in granular soil deposit under cyclic loading. The numerical model was verified by the centrifuge tests. The good match of the numerical results and the centrifuge experimental data shows that the fuzzy set model is an effective tool for assessing liquefaction potential and liquefaction-related motions.

Keywords Fuzzy-set plasticity · Sand liquefaction · Cyclic loading · Centrifuge modeling

Y. Bao
Department of Civil Engineering Technology, Environmental Management and Safety, Rochester Institute of Technology, CST-3151, 78 Lomb Memorial Drive, Rochester, NY 14623, USA
e-mail: axbite@rit.edu

S. Sture (✉)
Vice Chancellor for Research, 26 UCB, University of Colorado at Boulder, Boulder, CO 80309-026, USA
e-mail: stein.sture@colorado.edu

1 Introduction

Liquefaction-induced deformation and spreading phenomena have been observed in many recorded earthquakes. Strong-motion data also show a strong relationship between soil dilation or contraction at large cyclic shear strain excursions. Soil dilation phases can cause significant increases in shear stiffness and strength, and subsequently lead to a strong restraining effect on the magnitude of cyclic and accumulated permanent shear strains, while soil contraction typically leads to liquefaction. A granular soil shows strongly coupled shear-dilation behavior under cyclic loading. In a saturated soil, the shear induced dilation or contraction results in the migration of fluid into or from the pore-space. This migration process will be retarded by lower soil permeability or increased rate of loading, and thus lead to pore water pressure generation and the associated changes in effective confinement. The pioneering experimental work related to the liquefaction phenomenon and cyclic mobility was attributed to Seed and Lee [14], Casagrande [4], Castro [5], Castro and Poulos [6] and Seed [15]. While the physical phenomenon is well understood, analytical modeling of soil liquefaction and computer simulation remain a challenge in that the development of constitutive models capable of predicting soil liquefaction has been lagging.

Fuzzy-set elasto-plasticity concepts were first proposed by Klisinski et al. [10], and the model has received increasing attention due to its versatility and simplicity. In this paper, an enhanced kinematic and cyclic plasticity model based on the concept of fuzzy-set plasticity was implemented to simulate realistic sand behavior during unloading and reloading cycles. The enhanced model is not only capable of capturing the general nonlinear behavior of soil, but also the essential soil characteristics including pressure sensitivity, soil skeleton contraction and dilation, critical state soil mechanics features and pore pressure build-up. The enhanced fuzzy set model is based on simple and explicit formulations [3].

Many cyclic constitutive models provide tensorial incremental stress–strain relations for the deviatoric component and provide the volumetric response as a special enhancement or independent expression. In these cases, deviatoric–volumetric coupling may be partial or nonexistent. On the other hand, the enhanced fuzzy-set model gives the tensorial incremental stress–strain relation for all components, and deals with deviatoric–volumetric coupling in a consistent manner. The fuzzy-set model is capable of simulating shear induced volume changes by applying the dilatancy parameters under cyclic loading and predicting pore water pressure buildup in a rational way.

Before the advent of centrifuge modeling, verification of numerical simulations of earthquake-induced phenomena was a major challenge due to the lack of field data and the difficulties in replicating the full scale earthquake event during liquefaction in laboratory testing. Centrifuge modeling of seismic problems has been one of the most important experimental techniques to study the full scale strong-motion performance of earth structures as well as an effective means to validate numerical models. In dynamic centrifuge modeling, which has been described by Ko [11], scaled models can be prepared with desired geometry profiles and soil properties. The shake table mounted on the in-flight platform of centrifuges can apply controllable input base motions, which make centrifuge modeling particularly suitable to study fundamental issues related to seismic problems [7].

2 Fuzzy-set cyclic plasticity model

Fuzzy-set plasticity borrows the term "fuzzy-set" from probability theory, it is assumed that there exists an ultimate yield surface, where the behavior of the material is entirely plastic [8]. In addition, the material behavior inside the initial yield surface is purely elastic. The elasto-plastic response between the initial and the ultimate yield surfaces is characterized by a fuzzy set, where a real number $\gamma(\boldsymbol{\sigma})$ on the interval of 0–1 can be assigned to each point $\boldsymbol{\sigma}$ represented by the stress state in the region $F < 0$, where F is the yield function. The membership function $\gamma(\boldsymbol{\sigma})$ for the fuzzy set $F \leq 0$ represents the "membership degree" of the stress $\boldsymbol{\sigma}$ to the set of purely elastic material behavior as shown in Fig. 1. The plastic modulus is defined in terms of the value of a membership function [8, 10].

The strain increment $d\boldsymbol{\varepsilon}$ in the deviatoric–volumetric space can be described as follows:

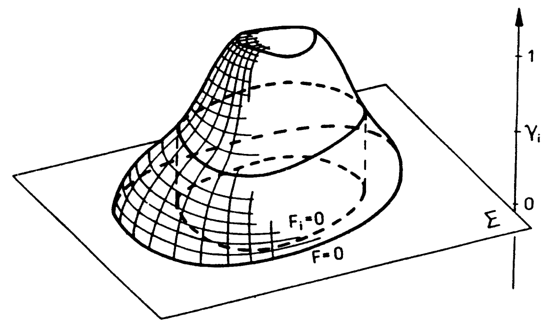

Fig. 1 "Fuzzy" yield surface specified by a given constant value of the membership function (Klisinski [10])

$$d\boldsymbol{\varepsilon} = d\boldsymbol{\varepsilon}^e + d\boldsymbol{\varepsilon}^p = d\boldsymbol{\varepsilon}^e + d\boldsymbol{\varepsilon}_d^p + d\boldsymbol{\varepsilon}_v^p = \begin{Bmatrix} d\varepsilon_v \\ d\varepsilon_d \end{Bmatrix} \quad (1)$$

where the superscript e denotes "elastic", the superscript p denotes "plastic", the subscript d denotes "deviatoric", and the subscript v denotes "volumetric".

$$d\boldsymbol{\varepsilon}^e = \mathbf{C}^e d\boldsymbol{\sigma} = \begin{bmatrix} \frac{1}{K} & 0 \\ 0 & \frac{1}{3G} \end{bmatrix} \begin{Bmatrix} dp \\ dq \end{Bmatrix} \quad (2)$$

where p and q are mean effective stress and deviatoric stress, respectively

$$d\boldsymbol{\varepsilon}_d^p = \mathbf{C}_d^p d\boldsymbol{\sigma} = \frac{1}{H_d} \mathbf{m}_d \mathbf{n}_d^T d\boldsymbol{\sigma} \quad (3)$$

where $H_d = \left(\frac{M_d \gamma_d^{s_d}}{1-\gamma_d^{s_d+1}}\right)\left(\frac{p}{p_0}\right)^{n_p}$ is the deviatoric plastic modulus, in which $\gamma_d \in [0, 1]$ is the deviatoric membership function, and M_d, s_d and n_p are model parameters. $\mathbf{n}_d$ is the normal tensor of the deviatoric loading surface and $\mathbf{m}_d = \mathbf{T}\mathbf{n}_d$ is the flow direction. The transformation matrix $\mathbf{T}$ is introduced to apply a non-associated flow rule to the deviatoric part of the plastic deformation [9].

$$\mathbf{T} = \begin{bmatrix} B & 0 \\ 0 & 1 \end{bmatrix} \quad (4)$$

where B is the dilatancy parameter that controls the soil dilatancy behavior in the model.

The deviatoric ultimate yield surface can be described as

$$F_d = g(\theta)q - a_0 - a_1 p \quad (5)$$

where $a_1 = M_c + \kappa\langle -\psi \rangle$, a_0 is a material constant related to soil cohesion, and θ is the Lode angle. The "elliptical" function $g(\theta)$ determines the shape of the trace of the ultimate yield surface in any deviatoric plane and is attributed to Willam and Warnke [16].

The state parameter ψ is defined as the difference between the current void ratio and the critical void ratio, i.e. $\psi = e - e_c$. For loose soil, $\psi > 0$; and for dense soil, $\psi < 0$.

The Phase Transformation Surface (PTS) is the stress points at which the volumetric changes of sands transform from contraction to dilation [17]. The existence of PTS is critical to understanding the cyclic pore water pressure variation in cyclic mobility.

The effective stress ratio is defined as

$$\eta = \frac{q}{p} \tag{6}$$

On PTS, $\eta = \eta_{PT}$: no volumetric change takes place, the mean effective confining stress p remains constant and no pore water pressure generation.

Below PTS, $\eta < \eta_{PT}$: contraction takes place, pore water pressure increases and the mean effective confining stress p decreases.

Above PTS, $\eta > \eta_{PT}$: dilation takes place, pore water pressure decreases and the mean effective confining stress p increases.

The coupled shear-dilatancy mainly relates to: current effective stress ratio η; state parameter ψ; and loading, unloading and reloading conditions.

An exponential expression for "B" was proposed in [3]:

Loading and reloading:

$$B = \alpha_1|\psi|\left[\exp\left(1 - \frac{|\eta|}{|\eta_{PT}|}\right) - 1\right], \quad \eta < \eta_{PT} \tag{7}$$

$$B = \alpha_2|\psi|\left[\exp\left(\frac{|\eta| - |\eta_{PT}|}{|\eta_F| - |\eta_{PT}|}\right) - 1\right], \quad \eta > \eta_{PT} \tag{8}$$

Unloading:

$$B = \beta|\psi|\exp\left(\frac{|\eta|}{|\eta_F|}\right) \tag{9}$$

where α_1, α_2 and β are model parameters, and η_F is the effective stress ratio at failure.

$\mathbf{n}_d$ describes the normal to the deviatoric loading surface, thus

$$\mathbf{n}_d = \frac{1}{\sqrt{\left(\frac{\partial F_d}{\partial p}\right)^2 + \left(\frac{\partial F_d}{\partial q}\right)^2}}\begin{Bmatrix} \frac{\partial F_d}{\partial p} \\ \frac{\partial F_d}{\partial q} \end{Bmatrix} = \frac{1}{\sqrt{a_1^2 + g^2(\theta)}}\begin{Bmatrix} -a_1 \\ g(\theta) \end{Bmatrix} \tag{10}$$

A non-associative flow rule is used for the deviatoric plastic deformation, and the flow direction $\mathbf{m}_d$ is defined as.

$$\begin{aligned}\mathbf{m}_d &= \mathbf{T}\mathbf{n}_d \\ &= \begin{bmatrix} B & 0 \\ 0 & 1 \end{bmatrix}\frac{1}{\sqrt{a_1^2 + g^2(\theta)}}\begin{Bmatrix} -a_1 \\ g(\theta) \end{Bmatrix} \\ &= \frac{1}{\sqrt{a_1^2 + g^2(\theta)}}\begin{Bmatrix} -a_1 B \\ g(\theta) \end{Bmatrix}\end{aligned} \tag{11}$$

$$\begin{aligned}\mathbf{C}_d^p &= \frac{1}{H_d}\mathbf{m}_d\mathbf{n}_d^T \\ &= \frac{1}{H_d}\frac{1}{a_1^2 + g^2(\theta)}\begin{bmatrix} a_1^2 B & -a_1 g(\theta)B \\ -a_1 g(\theta) & g^2(\theta) \end{bmatrix}\end{aligned} \tag{12}$$

The volumetric ultimate yield surface can be expressed as

$$F_v = p - p_e \tag{13}$$

$$d\varepsilon_v^p = \mathbf{C}_v^p d\boldsymbol{\sigma} = \frac{1}{H_v}\mathbf{m}_v\mathbf{n}_v^T d\boldsymbol{\sigma} \tag{14}$$

where $\mathbf{n}_v$ represents the normal to the volumetric loading surface,

$$\mathbf{n}_v = \frac{1}{\sqrt{\left(\frac{\partial F_v}{\partial p}\right)^2 + \left(\frac{\partial F_v}{\partial q}\right)^2}}\begin{Bmatrix} \frac{\partial F_v}{\partial p} \\ \frac{\partial F_v}{\partial q} \end{Bmatrix} = \begin{Bmatrix} 1 \\ 0 \end{Bmatrix} \tag{15}$$

An associated flow rule is used for the volumetric stress–strain relationship, and therefore, $\mathbf{m}_v = \mathbf{n}_v$.

$H_v = \left(\frac{M_v\gamma_v^{s_v}}{1-\gamma_v^{s_v+1}}\right)\left(\frac{p}{p_0}\right)^{n_p}$, is the volumetric plastic modulus, in which $\gamma_v \in (0, 1)$ is the volumetric membership function; M_v and s_v are model parameters.

$$\mathbf{C}_v^p = \frac{1}{H_v}\begin{bmatrix} 1 & 0 \\ 0 & 0 \end{bmatrix} \tag{16}$$

Thus, the explicit expression for the fuzzy set plasticity model is [3],

$$\begin{aligned} d\boldsymbol{\varepsilon} = \mathbf{C}^{ep}d\boldsymbol{\sigma} = \Bigg(&\begin{bmatrix} \frac{1}{K} & 0 \\ 0 & \frac{1}{3G} \end{bmatrix} \\ &+ \frac{1}{H_d}\frac{1}{a_1^2 + g^2(\theta)}\begin{bmatrix} a_1^2 & -a_1 g(\theta)B \\ 0 & g^2(\theta) \end{bmatrix} \\ &+ \frac{1}{H_v}\begin{bmatrix} 1 & 0 \\ 0 & 0 \end{bmatrix}\Bigg)\begin{Bmatrix} dp \\ dq \end{Bmatrix}\end{aligned} \tag{17}$$

The model capabilities were mainly focused on deviatoric–volumetric strain coupling under undrained conditions during cyclic loading. Undrained conditions are considered as the predominant loading condition leading to soil liquefaction. Volumetric changes in the soil skeleton depend on the loading history. Contraction results in a pore water pressure increase, which reduces the soil strength and elastic stiffness moduli, while dilation leads to regain of shear stiffness and strength, and therefore restrains the magnitude of pore water pressure.

3 Centrifuge model preparation

Centrifuge modeling has been considered among the best experimental methods for modeling soil liquefaction and observing phenomena. It creates stress conditions in the model that closely simulate those in the full-scale prototype, so that the behavior of the model can approximate that of the prototype. Since 1988, University of Colorado at Boulder has operated a 400 g-ton centrifuge. A servo-controlled electro-hydraulic shake table is mounted on a platform that is capable of swinging in the inertia field of the centrifuge, which could be operated inflight to produce earthquake-like motions. In this study, the centrifuge and the shake table were used to test models of a layer of 10 m thick in a prototype liquefiable soil stratum. The pore water pressure and acceleration at different elevations were measured and the settlement of soil surface was also recorded. The model was constructed at 40-th scale, and the centrifuge was spun at 40 g to simulate appropriate prototype behavior. The model was saturated with a viscous liquid comprising of a metolose solution having a viscosity 40 times greater than the viscosity of water to ensure appropriate scaling between dynamic and diffusion phenomena of the given g-level. Absorbing boundaries using cork plates in the shaking direction were adopted to simulate the infinite boundary conditions presented in the prototype.

The dimensions of the aluminum container were 406 mm (L) × 216 mm (W) × 343 mm (H). Two 12.7 mm thick cork plates were attached to each end of the container in the shaking direction to reduce the reflection effect due to the rigid walls of the container. The input base acceleration comprised of a cyclic motion with amplitude of 0.2 g, frequency of 1 Hz and 10 s time duration in the prototype scale. Five pore pressure transducers were used in the experiment, and they were located at a depth of 2, 4, 6, 8 and 9.6 m from the surface. Seven accelerometers were used; two at the base to measure the input horizontal and vertical accelerations and the other five were embedded in the sand layer. The five accelerometers in the sand layer were located at the surface, at the depth of 2, 4, 6 and 8 m from the surface, respectively. One LVDT was located on the surface to measure the settlement. The model cross-section and the layout of instrumentation are shown in Fig. 2.

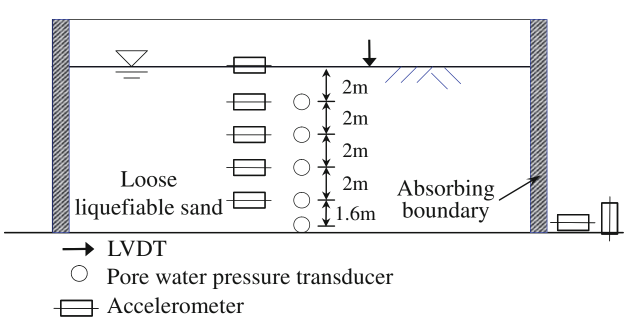

Fig. 2 Cross-section of the centrifuge model and instrumentation layout

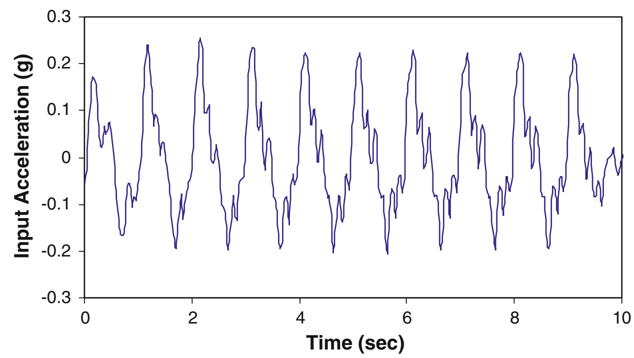

Fig. 3 Input motions: horizontal acceleration

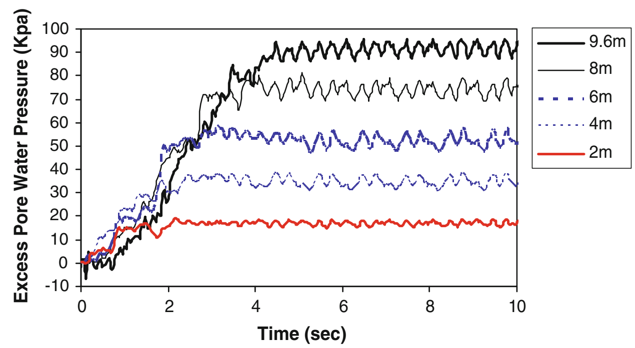

Fig. 4 Measured excess pore water pressure at different depths in the sand layer

The sand used in the centrifuge experiments was Nevada sand No. 120. Nevada sand No. 120 is classified as fine sand and the initial void ratio of the soil was measured at 0.776. According to the data tested by Arulmoli et al. [1], the maximum void ratio of Nevada Sand is 0.887 and the minimum void ratio is 0.511, therefore, the initial relative density of the soil as placed in the container was 30%. Soil unit weight is 19.7 KN/m^3, and buoyancy unit weight is 9.9 KN/m^3.

The soil stratum was prepared by the sedimentation method, in which the soil was deposited in the metolose solution by its self weight. The real-time shake table input base acceleration in the prototype scale is shown in Fig. 3.

The excess pore water pressure records of the prototype scale during and after the shaking event are displayed in Fig. 4.

4 Numerical modeling of the layer of soil at 9.6 m subjected to cyclic loading

At the layer of 9.6 m, the total mean stress keeps constant of 95 kPa and the deviatoric stress increases gradually from 0 to 19 kPa, which is corresponding to horizontal acceleration = 0.2 g, unloads to 0, and reloads to 19 kPa, and the amplitude of deviatoric stress keeps constant for 10 cycles. The loading history is shown in Fig. 5 and the model responses are shown in Figs. 6, 7, 8.

Model parameters are listed in Table 1. The numerical model has 16 parameters, and these parameters can be classified into three categories. There are ten fuzzy-set parameters: K_0, G_0, n_p, p_e, M_d, s_d, M_l, s_l, γ_{dF} and γ_{l0}; three critical state parameters: e_c, φ_F and φ_{PT} and three dilatancy parameters. The model parameters were calibrated using unconstrained numerical optimization. The unconstrained numerical optimization technique involves comparison between laboratory data and numerical simulations. An objective function was constructed by summing the distance norm between laboratory data and numerical simulation. Random search method was adopted to calibrate the model parameters due to its easy implementation [2]. Conventional triaxial test and isotropic compression test were used for calibrating fuzzy set parameters. Consolidation test was conducted to calibrate the critical state parameters and cyclic triaxial tests were conducted to calibrate the dilatancy parameters.

The computed model responses agree with the centrifuge modeling test data very well and are consistent with a large number of undrained laboratory experiments, which have been used to study the cyclic behavior of sands [4–6, 12, 13, 14].

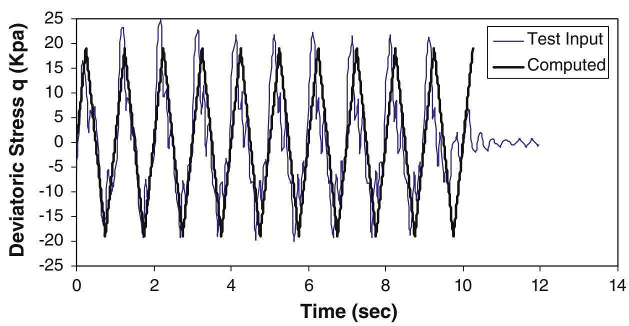

Fig. 5 Loading history of deviatoric stress

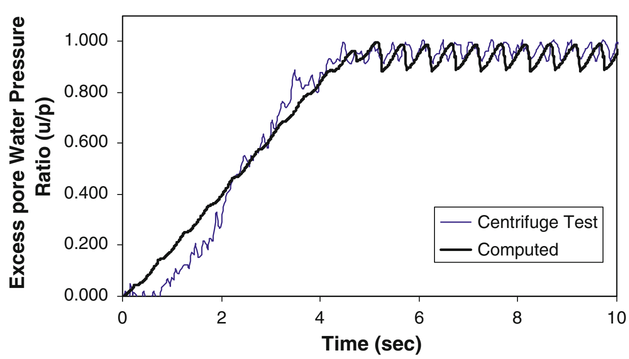

Fig. 6 Pore water pressure buildup history

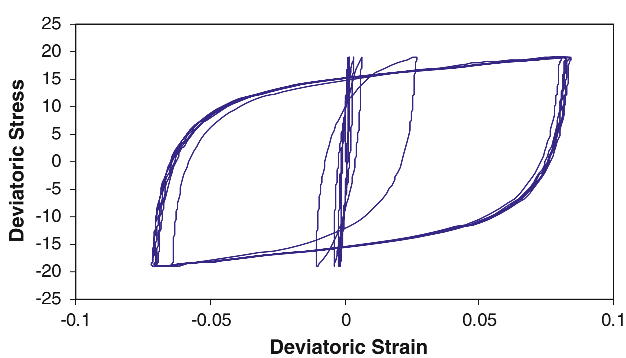

Fig. 7 Computed deviatoric stress–strain curve

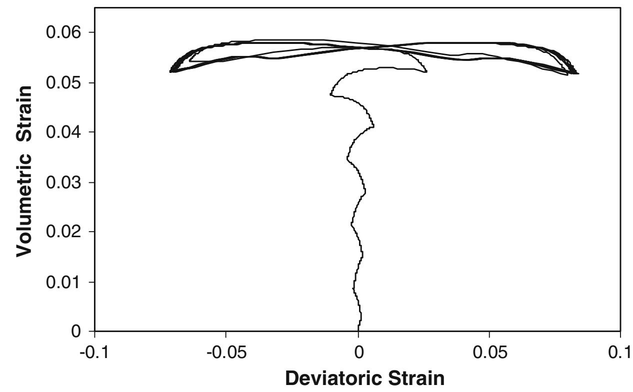

Fig. 8 Computed volumetric strain–deviatoric strain response

Table 1 Fuzzy-set model parameters

Fuzzy-set parameters	
Reference bulk modulus K_0 (kPa)	13831
Reference shear modulus G_0 (kPa)	5028
Reference mean pressure p_0 (kPa)	95
Pressure dependence coefficient n_p	0.5
Locking mean pressure p_e (kPa)	12657
Deviatoric plastic modulus coefficient M_d (kPa)	387000
Deviatoric plastic modulus coefficient s_d	2.1415
Locking plastic modulus coefficient M_l (kPa)	160100
Locking plastic modulus coefficient s_l	1.6472
Deviatoric failure membership function γ_{dF}	0.05
Locking membership at the mean pressure of “0” γ_{l0}	0.20
Critical state parameters	
Initial void ratio e_0	0.776
Critical void ratio e_c	0.650
Angle of failure line φ_F (°)	40
Angle of phase transformation line φ_{PT} (°)	30
Dilatancy parameters	
Contraction parameter under loading α_1	−15
Dilation parameter under loading α_2	13
Contraction parameter under unloading β	28

Under undrained conditions, the dilatancy induced volume increase leads to an immediate reduction in pore water pressure and associated increase in effective confinement. The enhanced fuzzy set model successfully captures the features of progressive pore water pressure build-up and cyclic pore water pressure variations under cyclic shear loading, as shown in Fig. 6. The cyclic deviatoric stress–strain curves, as shown in Fig. 7, describe a cycle-by-cycle degradation in strength. Pore water pressure build-up is directly related to the volume change of soil skeleton. Fig. 8 shows that the volume change of soil skeleton increases cycle by cycle and tends to approach a steady state value.

5 Conclusions

A kinematic and cyclic plasticity model based on fundamental mechanics principles and fuzzy set elasto-plasticity theory was implemented to simulate sand liquefaction under cyclic loading.

The enhanced fuzzy set model accurately predicts the volumetric changes of soil skeleton by introducing the soil dilatancy parameter.

The model is a useful tool to understand the mechanism of soil liquefaction under earthquake and the model is capable of capturing the important features of cyclic pore water pressure build-up under undrained conditions.

Centrifuge modeling experiments and numerical simulation of a liquefiable sand layer are conducted and compared. Both the numerical and experimental results show that the development of pore water pressure and liquefaction are a consequence of the base excitation. The computed results showed good match with the experimental data. The capability of the enhanced fuzzy-set model in simulating soil liquefaction is validated. The developed fuzzy-set plasticity formulation and computational procedure are an effective means to assess liquefaction potential and liquefaction-related deformations.

References

1. Arulmoli, K., Muraleetharan, K.K., Hossain, M.M., Fruth, L.S.: VELACS Laboratory Testing Program, Soil Data Report. The Earth Technology Corporation, Project No. 90–0562. Irvine, California (1992)
2. Bao, Y., Ge, Y.-N., Sture, S.: Unconstrained optimization and calibration of a kinematic-cyclic plasticity model. ASCE Geotechnical Special Publication No. 128, Soil Constitutive Models—Evaluation, Selection, and Calibration, 45–68, Geo-Frontiers 2005. Austin, Texas (2005)
3. Bao, Y., Ge, Y.-N., Sture, S., Ko, H.-Y.: Numerical modeling of cyclic mobility in saturated soil. In: Proceedings of 3rd Biot Conference on Poromechanics, pp. 353–359. Norman, Oklahoma (2005)
4. Casagrande, A.: Memorandum titled "Terminology concerning cyclic tests". June 11, 1969
5. Castro, G.: Liquefaction and cyclic mobility of saturated sands. J. Geotech. Eng. ASCE, 101, GT6, 551–569 (1975)
6. Castro, G., Poulos, S.J.: Factors affecting liquefaction and cyclic mobility. J. Geotech. Eng. ASCE, 103, GT6, 501–516 (1977)
7. Ge, L., Bao, Y., Ni, C.K., Ko, H.Y.: Seismic centrifuge modelling of earth dams. Geomech. Geoeng. **5**(4), 247–257 (2010)
8. Klisinski, M.: Plasticity theory based on fuzzy sets. J. Eng. Mech. ASCE **114**(4), 563–582 (1988)
9. Klisinski, M., Abifadel, N., Runesson, K., Sture, S.: Modeling of the behavior of dry sand by an elasto-plastic 'fuzzy set' model. Comput. Geotech. **11**, 229–261 (1991)
10. Klisinski, M., Alawi, M.M., Sture, S., Ko, H.-Y., Muir Wood, D.: Elasto-plastic model for sand based on fuzzy sets. In: International Workshop on Constitutive Equations for Granular Non-Cohesive Soils. Case Western Reserve University (1987)
11. Ko, H.Y.: Modeling of seismic problems in centrifuges. In: Leung, C.F., Lee, F.H., Tan, T.S. (eds.) Proceedings of Centrifuge 94, pp. 3–12. Balkema, Rotterdam (1994)
12. Koga, Y., Matsuo, O.: Shaking table tests of embankments resting on liquefiable sandy ground. Soils Found. **30**(4), 162–174 (1990)
13. Krstelj, I., Prevost, J.H.: Dynamic effects in a saturated layered soil deposit: centrifuge modeling. Soil Dyn. Earthq. Eng. **11**, 485–496 (1992)
14. Seed, H.B., Lee, K.L.: Liquefaction of saturated sands during cyclic loading. J. Soil Mech. Found. Divis. ASCE, 92, SM6, 105–134 (1966)
15. Seed, H.B.: Soil liquefaction and cyclic mobility evaluation for level ground during earthquakes. J. Geotech. Eng. Divis. ASCE, 105, GT2, 201–255 (1979)
16. Willam, K.J., Warnke, E.P.: Constitutive model for the triaxial behavior of concrete. Seminar on Concrete Structures Subjected to Triaxial Stresses. ISMES, Bergamo, Italy, 1974, Published in IABSE Report 19, Zurich III-I (1975)
17. Zhang, J.M., Shamoto, Y., Tokimatsu, K.: Moving critical and phase transformation stress state lines of saturated sands during undrained cyclic shear. Soils Found. **37**(2), 51–59 (1997)